Modeling the Optical Interaction Between a Carbon Nanotube and a Plasmon Resonant Sphere

George W. Hanson, *Senior Member, IEEE*, and Paul Smith

***Abstract*—A model is presented for the electromagnetic interaction between a carbon nanotube and an electrically-small sphere, such as a plasmonic metal particle. The sphere is characterized by its dipole moment, which is coupled to an integral equation for the nanotube. The model can be easily adapted to other systems consisting of electrically-small objects coupled to larger objects requiring a full-wave treatment. It is found that the presence of a nonplasmonic electrically-small sphere has a small effect on observed system properties, but that a plasmonic nanosphere in close proximity to a carbon nanotube leads to pronounced coupling, and may be useful as a way to excite carbon nanotube antennas. Furthermore, backscattering from a plasmonic nanosphere-carbon nanotube system is dominated by the nanosphere response. An approximate analytical solution is provided for the current induced on a nanotube in the presence of a plasmonic nanosphere.**

***Index Terms*—Carbon nanotubes, electromagnetic theory, nanosphere, nanotechnology, optical antenna, plasmons.**

I. Introduction

A CARBON nanotube [1] is a fundamental structure in nanoelectronics, with applications in diverse fields. In particular, semiconducting nanotubes can be used as transistors [2], [3] and related devices, and metallic tubes are envisioned as transmission lines [4]–[7] and antennas [8]–[14]. It is therefore important to understand the interaction between an electromagnetic wave and a carbon nanotube, and electromagnetic interaction effects among nanotubes and with other nanostructures.

A second nanostructure of fundamental importance is a plasmonic nanoparticle, such as a nanoscopic noble metal spheroid at optical frequencies. Plasmonic nanoparticles have formed an area of intense study in recent years for a number of reasons, such as their use in forming subwavelength optical devices [15]–[17] and in biological/medical applications [18]. The importance of particle plasmons is due to their intense near-field, which can enhance electromagnetic effects by several orders of magnitude [19]–[21].

In this paper, the electromagnetic interaction between a carbon nanotube and a plasmonic nanoparticle is studied. The carbon nanotube is modeled using an integral equation involving a quantum mechanical surface conductance, and the electrically-small nanoparticle is characterized by its dipole moment, leading to a relatively simple and efficient formulation. The use of an integral equation for the nanotube is necessary, since its length is an appreciable fraction of a wavelength at the considered frequencies. One possible application of the considered system is to carbon nanotube optical antennas, where, for example, an incident plane wave can excite the nanotube-nanoparticle system. If the nanoparticle undergoes a plasmonic resonance, it can provide a strong localized excitation for the carbon nanotube antenna, inducing more current to flow on the antenna than if the nanoparticle were absent. In the following, all units are in the SI system, and the time variation (suppressed) is $e^{j\omega t}$.

Manuscript received August 24, 2006; revised January 17, 2007.

G. W. Hanson is with the Department of Electrical Engineering, University of Wisconsin-Milwaukee, Milwaukee, WI 53211 USA (e-mail: george@uwm.edu).

P. Smith is with the Department of Mathematics, Macquarie University, NSW 2109, Australia.

Color versions of one or more of the figures in this paper are available online at http://ieeexplore.ieee.org.

Digital Object Identifier 10.1109/TAP.2007.908555

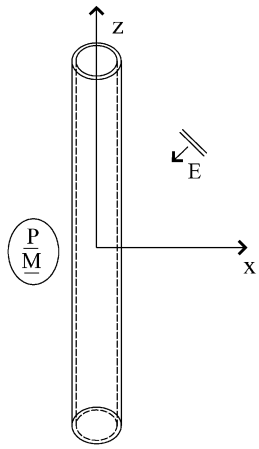

Fig. 1. Carbon nanotube in close proximity to an electrically-small object modeled by its electric and magnetic polarizabilities $\underline{\mathbf{P}}$ and $\underline{\mathbf{M}}$.

II. Formulation

The formulation is developed for a carbon nanotube coupled to an electrically-small polarizable object characterized by its electric and magnetic polarizabilities, as depicted in Fig. 1, but it can be easily extended to larger coupled systems. Following [9]–[13], the carbon nanotube is modeled as a finite length hollow cylinder with an infinitely-thin wall, characterized by a surface conductance σ_{cn}. In general, carbon nanotubes are characterized by the dual index (m,n), where $(m,0)$ for zigzag CNs, (m,m) for armchair CNs, and (m,n), $0 < n \neq m$, for chiral nanotubes. Interestingly, carbon nanotubes can be either metallic or semiconducting, depending on their geometry (i.e., on m,n) [22]. Armchair CNs are always metallic (they exhibit no energy bandgap), as are zigzag CNs with $m = 3q$, where q is an integer (although zigzag tubes can have a small bandgap due to curvature effects, one can usually consider them as metallic from an applications perspective). The resulting cross-sectional radius of a carbon nanotube is given by [22]

$$a = \frac{\sqrt{3}}{2\pi} b \sqrt{m^2 + mn + n^2} \tag{1}$$

where $b = 0.142$ nm is the interatomic distance in graphene.

A. Development of the Model

Starting with Maxwell's equations

$$\nabla \times \mathbf{E}(\mathbf{r}) = -j\omega\mu\mathbf{H}(\mathbf{r}) - \mathbf{J}_m(\mathbf{r}) \tag{2}$$
$$\nabla \times \mathbf{H}(\mathbf{r}) = j\omega\varepsilon\mathbf{E}(\mathbf{r}) + \mathbf{J}_e(\mathbf{r}) \tag{3}$$

where μ and ε are material parameters of the space occupied by the nanotube-sphere system, and $\mathbf{J}_{e,m}$ are electric and magnetic current densities, respectively, solutions can be written as [23], [24]

$$\mathbf{E}(\mathbf{r}) = -j\omega\mu \int_\Omega \underline{\mathbf{G}}^{e,e}(\mathbf{r},\mathbf{r}') \cdot \mathbf{J}_e(\mathbf{r}')\, d\Omega' + \int_\Omega \underline{\mathbf{G}}^{e,m}(\mathbf{r},\mathbf{r}') \cdot \mathbf{J}_m(\mathbf{r}') d\Omega' \tag{4}$$

$$\mathbf{H}(\mathbf{r}) = -j\omega\varepsilon \int_\Omega \underline{\mathbf{G}}^{m,m}(\mathbf{r},\mathbf{r}') \cdot \mathbf{J}_m(\mathbf{r}') d\Omega' + \int_\Omega \underline{\mathbf{G}}^{m,e}(\mathbf{r},\mathbf{r}') \cdot \mathbf{J}_e(\mathbf{r}') d\Omega' \tag{5}$$

where [25]

$$\underline{\mathbf{G}}^{e,e}(\mathbf{r},\mathbf{r}') = \mathrm{P.V.}\left\{\frac{1}{\omega^2\mu}\underline{\mathbf{F}}^{e,e}(\mathbf{r},\mathbf{r}')\right\} - \frac{\underline{\mathbf{L}}\delta(\mathbf{r}-\mathbf{r}')}{k^2} = \underline{\mathbf{G}}^{m,m}(\mathbf{r},\mathbf{r}') \tag{6}$$

$$\underline{\mathbf{G}}^{e,m}(\mathbf{r},\mathbf{r}') = \frac{1}{j\omega\mu}\underline{\mathbf{F}}^{e,m}(\mathbf{r},\mathbf{r}') = -\underline{\mathbf{G}}^{m,e}(\mathbf{r},\mathbf{r}') \tag{7}$$

$k^2 = \omega^2\mu\varepsilon$, P.V. indicates that the associated term is to be integrated in the principal value sense [26], $\underline{\mathbf{L}}$ is the depolarizing dyadic, and Ω is the support of the current. Furthermore

$$\underline{\mathbf{F}}^{e,e}(\mathbf{r},\mathbf{r}') = \omega^2\mu\left[\underline{\mathbf{I}} + \frac{\nabla\nabla}{k^2}\right] g(\mathbf{r},\mathbf{r}') = g(\mathbf{r},\mathbf{r}')\left\{\left(3\hat{\mathbf{R}}\hat{\mathbf{R}} - \underline{\mathbf{I}}\right)\left(\frac{1}{\varepsilon R^2} + \frac{j\omega\eta}{R}\right) - (\hat{\mathbf{R}}\hat{\mathbf{R}} - \underline{\mathbf{I}})\omega^2\mu\right\} \tag{8}$$

$$\underline{\mathbf{F}}^{e,m}(\mathbf{r},\mathbf{r}') = F^{e,m}(\mathbf{r},\mathbf{r}')\hat{\mathbf{R}} \times \underline{\mathbf{I}} \tag{9}$$

$$F^{e,m}(\mathbf{r},\mathbf{r}') = g(\mathbf{r},\mathbf{r}')\left[-\frac{\omega^2\mu}{c} + \frac{j\omega\mu}{R(\mathbf{r},\mathbf{r}')}\right] \tag{10}$$

$$g(\mathbf{r},\mathbf{r}') = \frac{e^{-jkR(\mathbf{r},\mathbf{r}')}}{4\pi R(\mathbf{r},\mathbf{r}')} \tag{11}$$

where $\mathbf{R} = \mathbf{R}(\mathbf{r},\mathbf{r}') = \mathbf{r}-\mathbf{r}', R = R(\mathbf{r},\mathbf{r}') = |\mathbf{R}|, \hat{\mathbf{R}} = \mathbf{R}/R$, $\underline{\mathbf{I}}$ is the unit dyadic, and $c = 1/\sqrt{\mu\varepsilon}$.

It is assumed that the lossy dielectric object is electrically small, such that its maximum linear dimension is much less than the free-space wavelength and the wavelength inside the dielectric (yet much larger than the Fermi wavelength, so as to ignore quantum confinement effects). In this case the object can be represented by its electric and magnetic dipole moment [27], [28], $\mathbf{p}$ and $\mathbf{m}$, respectively. Associated currents are

$$\mathbf{J}_e = j\omega\mathbf{p}\delta(\mathbf{r} - \mathbf{r}_{dm}) \tag{12}$$
$$\mathbf{J}_m = j\omega\mu\mathbf{m}\delta(\mathbf{r} - \mathbf{r}_{dm}) \tag{13}$$

where $\mathbf{r}_{dm}$ is the location of the dipole moment

$$\mathbf{r}_{dm} = \hat{\mathbf{x}}x_{dm} + \hat{\mathbf{y}}y_{dm} + \hat{\mathbf{z}}z_{dm} \tag{14}$$

i.e., the polarizable object is centered at (x_{dm}, y_{dm}, z_{dm}). The fields due to the dipole moments are then

$$\mathbf{E}^{p,m}(\mathbf{r}) = \underline{\mathbf{F}}^{e,e}(\mathbf{r},\mathbf{r}_{dm}) \cdot \mathbf{p} + \underline{\mathbf{F}}^{e,m}(\mathbf{r},\mathbf{r}_{dm}) \cdot \mathbf{m} \tag{15}$$

$$\mathbf{H}^{p,m}(\mathbf{r}) = \varepsilon\underline{\mathbf{F}}^{e,e}(\mathbf{r},\mathbf{r}_{dm}) \cdot \mathbf{m} - \frac{1}{\mu}\underline{\mathbf{F}}^{e,m}(\mathbf{r},\mathbf{r}_{dm}) \cdot \mathbf{p}. \tag{16}$$

Since the carbon nanotube is modeled as a cylinder having an infinitely-thin wall and an electrically-small radius $a\,(ka \ll 1)$, current density on a carbon nanotube with axis coincident with the z-axis can be written as [10]

$$\mathbf{J}_e^{cn}(\rho,\phi,z) = \hat{\mathbf{z}}J_z^{cn}(z)\delta(\rho - a) \tag{17}$$

so that

$$I_{cn}(z) = \int_0^a \int_0^{2\pi} J_z^{cn}(z)\delta(\rho - a)\rho d\phi d\rho \tag{18}$$
$$= J_z^{cn}(z)2\pi a \tag{19}$$

leading to fields

$$\mathbf{E}^{cn}(\mathbf{r}) = \frac{1}{j4\pi\omega\varepsilon}(k^2 + \boldsymbol{\nabla}\boldsymbol{\nabla}\cdot)\hat{\mathbf{z}}\int_{-L}^{L}\int_{-\pi}^{\pi}\frac{e^{-jkR(\mathbf{r},\mathbf{r}'_{cn})}}{2\pi R(\mathbf{r},\mathbf{r}'_{cn})} \times I_{cn}(z')\, d\phi' dz' \tag{20}$$

$$\mathbf{H}^{cn}(\mathbf{r}) = \nabla \times \hat{\mathbf{z}}\int_{-L}^{L}\int_{-\pi}^{\pi}\frac{e^{-jkR(\mathbf{r},\mathbf{r}'_{cn})}}{4\pi R(\mathbf{r},\mathbf{r}'_{cn})}I_{cn}(z')d\phi' dz' \tag{21}$$

where

$$\mathbf{r}'_{cn} = \mathbf{r}_{cn}(\phi', z') = \hat{\mathbf{x}}(x_{cn} + a\cos\phi') + \hat{\mathbf{y}}(y_{cn} + a\sin\phi') + \hat{\mathbf{z}}(z_{cn} + z') \tag{22}$$

locates positions on the wall of the carbon nanotube, and where (x_{cn}, y_{cn}, z_{cn}) denotes the tube center.

The seven scalar unknowns $\mathbf{p}$, $\mathbf{m}$, and I_{cn} can be obtained self-consistently by enforcing conditions on the field. The first condition is Ohm's law for the carbon nanotube [9]–[13]

$$J_z^{cn}(a,\phi,z) = \sigma_{cn}E_z(a,\phi,z) \tag{23}$$

enforced on the tube wall, where E_z is the z-component of the total electric field and σ_{cn} is the nanotube conductance (S). For an armchair or zigzag carbon nanotube the π-electron tight-binding quantum conductance is given by [9], [29]

$$\sigma_{cn}(\omega) = \frac{je^2\omega}{\pi^2\hbar a}\left\{\frac{1}{\omega(\omega - j\nu)}\sum_{s=1}^{m}\int_{1stBZ}\frac{\partial F_c}{\partial p_z}\frac{\partial \mathcal{E}_c}{\partial p_z}dp_z + 2\sum_{s=1}^{m}\int_{1stBZ}\mathcal{E}_c|R_{vc}|^2\frac{F_c - F_v}{\hbar^2\omega(\omega - j\nu) - 4\mathcal{E}_c^2}dp_z\right\} \tag{24}$$

where e is the charge of an electron, $\nu = \tau^{-1}$ is the phenomenological relaxation frequency (τ being the relaxation time), $\hbar$ is the reduced Planck's constant, $F_{c,v}$ and $\mathcal{E}_{c,v}$ are the equilibrium Fermi distribution function and electron dispersion relation in the conduction or valance bands, respectively, and R_{vc} is the matrix element for the nanotube. Explicit expressions for these quantities are given in [30].

The second condition is that the total field at the location of the dipole moment, due to all currents in the system except those associated with the dipole moment itself, is related to the dipole moment through the polarizability dyadics

$$\begin{aligned} \mathbf{p} &= \varepsilon \underline{\mathbf{P}} \cdot \mathbf{E}(\mathbf{r}_{dm}) \\ \mathbf{m} &= \underline{\mathbf{M}} \cdot \mathbf{H}(\mathbf{r}_{dm}) \end{aligned} \tag{25}$$

where $\underline{\mathbf{P}}$ and $\underline{\mathbf{M}}$ are the electric and magnetic polarizability tensors of the object, respectively. Specializing to the case of a non-magnetic nanosphere in free space [27]

$$\underline{\mathbf{P}} = \underline{\mathbf{I}} P_0, \quad \underline{\mathbf{M}} = \underline{\mathbf{0}} \tag{26}$$

$$P_0 = 4\pi r_s^3 \frac{\varepsilon_r - 1}{\varepsilon_r + 2} \tag{27}$$

where r_s is the radius of the sphere and ε_r is the relative permittivity of the sphere material. For other shapes, such as spheroids, polarizability tensors are available in [27] (although for reasons discussed below, here we will only consider spheres). Enforcing the two field conditions (23) and (25) leads to the coupled equations

$$\frac{I_{cn}(\mathbf{r}_{cn})}{2\pi a} = \sigma_{cn}\left(E_z^{s,cn}(\mathbf{r}_{cn}) + E_z^{s,p}(\mathbf{r}_{cn}) + E_z^i(\mathbf{r}_{cn})\right) \tag{28}$$

$$\mathbf{p} = \varepsilon \underline{\mathbf{P}} \cdot \left(\mathbf{E}^{s,cn}(\mathbf{r}_{dm}) + \mathbf{E}^i(\mathbf{r}_{dm})\right) \tag{29}$$

where the first equation is enforced for all z on the nanotube (ϕ in $\mathbf{r}_{cn}$ (22) can be set to zero because the nanotube current is assumed to be ϕ-independent, since $ka \ll 1$), $\mathbf{E}^{s,cn}$ is the electric field maintained by currents on the carbon nanotube, $\mathbf{E}^{s,p}$ is the field maintained by the electric dipole moment, and $\mathbf{E}^i$ is the incident field, i.e., the field that would be present in the absence of the carbon nanotube and the polarizable object. Explicitly, (28) becomes

$$\begin{aligned} \frac{I_{cn}(\mathbf{r}_{cn})}{2\pi a \sigma_{cn}} &= \frac{1}{j4\pi\omega\varepsilon}\left(k^2 + \frac{\partial^2}{\partial z^2}\right) \\ &\quad \times \int_{-L}^{L}\int_{-\pi}^{\pi} \frac{e^{-jkR_1}}{2\pi R_1} I_{cn}(z')\,d\phi'\,dz' \\ &\quad + \hat{\mathbf{z}} \cdot \underline{\mathbf{F}}^{e,e}(\mathbf{r}_{cn}, \mathbf{r}_{dm}) \cdot \mathbf{p} + E_z^i(\mathbf{r}_{cn}) \end{aligned} \tag{30}$$

$$\begin{aligned} \mathbf{p} &= \varepsilon \underline{\mathbf{P}} \cdot \frac{1}{j4\pi\omega\varepsilon}(k^2 + \nabla\nabla\cdot)\hat{\mathbf{z}} \\ &\quad \times \int_{-L}^{L}\int_{-\pi}^{\pi} \frac{e^{-jkR_2}}{2\pi R_2} I_{cn}(z')\,d\phi'\,dz' + \varepsilon \underline{\mathbf{P}} \cdot \mathbf{E}^i(\mathbf{r}_{dm}) \end{aligned} \tag{31}$$

where the first equation is enforced for all z on the nanotube, and where

$$\begin{aligned} R_1 &= R(\mathbf{r}_{cn}, \mathbf{r}'_{cn}) = \sqrt{(z - z')^2 + 4a^2 \sin^2(\phi'/2)}, \\ R_2 &= R(\mathbf{r}_{dm}, \mathbf{r}'_{cn}) \\ &= \sqrt{(z_{dm} - z')^2 + (x_{dm} - a\cos\phi')^2 + (y_{dm} - a\sin\phi')^2}. \end{aligned} \tag{32}$$

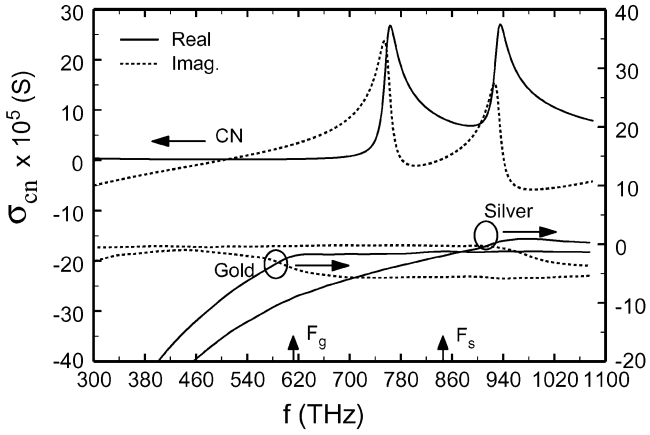

Fig. 2. Frequency-dependent material parameters for a (9, 0) carbon nanotube (σ_{cn} is the upper two curves showing interband transitions, corresponding to the left vertical axis) and bulk gold and silver (relative permittivity is given by the lower four curves, corresponding to the right vertical axis). The short arrows at $F_g = 612$ THz and $F_s = 846$ THz indicate the frequency where $\mathrm{Re}(\varepsilon_{\mathrm{gold}}) = -2\varepsilon_0$ and $\mathrm{Re}(\varepsilon_{\mathrm{silver}}) = -2\varepsilon_0$, respectively.

For computation it is convenient to remove the operator $(k^2 + \partial^2/\partial z^2)$ from (30) (the second derivative operator in (31) is not a problem since the derivatives can be moved inside the integral and evaluated). This leads to the Hallén form

$$\begin{aligned} &\int_{-L}^{L}\int_{-\pi}^{\pi}\left\{\frac{e^{-jkR_1}}{2\pi R_1} + f(z - z')\right\} I_{cn}(z')\,d\phi'\,dz' \\ &\quad = d_1 \sin kz + d_2 \cos kz \\ &\qquad - \frac{j4\pi\omega\varepsilon}{k}\int_{-L}^{z} \hat{\mathbf{z}} \cdot \underline{\mathbf{F}}^{e,e}(\mathbf{r}'_{cn}, \mathbf{r}_{dm}) \cdot \mathbf{p} \sin(k(z - z'))\,dz' \\ &\qquad - \frac{j4\pi\omega\varepsilon}{k}\int_{-L}^{z} E_z^i(\mathbf{r}'_{cn}) \sin(k(z - z'))\,dz' \end{aligned} \tag{33}$$

$$\begin{aligned} &\mathbf{p} - \frac{1}{j4\pi\omega}\underline{\mathbf{P}} \cdot (k^2 + \nabla\nabla\cdot)\hat{\mathbf{z}} \int_{-L}^{L}\int_{-\pi}^{\pi} \frac{e^{-jkR_2}}{2\pi R_2} I_{cn}(z')\,d\phi'\,dz' \\ &\quad = \varepsilon \underline{\mathbf{P}} \cdot \mathbf{E}^i(\mathbf{r}_{dm}) \end{aligned} \tag{34}$$

where the first equation is enforced for all z on the nanotube, d_1 and d_2 are constants to be determined upon setting the currents on the ends of the nanotubes to be zero, $I_{cn}(z_{cn} \pm L) = 0$, and where [10]

$$f(z - z') = \frac{\omega\varepsilon}{a\sigma_{cn}} \frac{e^{-jk|z - z'|}}{k}. \tag{35}$$

The incident field is assumed to be a uniform plane wave

$$\mathbf{E}^i(\mathbf{r}) = \mathbf{E}_0 e^{-jk(x \sin\theta\cos\phi + y\sin\theta\sin\phi + z\cos\theta)} \tag{36}$$

and a pulse function expansion, point matching method-of-moments solution, as described in [10], is used to solve (33).

B. Analytical Expression for the Carbon Nanotube Current

The carbon nanotube conductance σ_{cn} is quite small at optical frequencies, on the order of 10^{-5} (S), as will be shown in Fig. 2. Therefore, concerning the two terms involving I_{cn} in (30), the left side of the equality will be dominant over the first term on the right side. Furthermore, since the plasmon resonance is a strong phenomena, to a first approximation we

may neglect the influence of the carbon nanotube current on the dipole moment [i.e., the first term on the right side of (31)], and therefore, (30) and (31) can be simplified and combined to yield

$$\frac{I_{cn}(\mathbf{r}_{cn})}{2\pi a\sigma_{cn}} = \hat{\mathbf{z}}\cdot\underline{\mathbf{F}}^{e,e}(\mathbf{r}_{cn},\mathbf{r}_{dm})\cdot\varepsilon\underline{\mathbf{P}}\cdot\mathbf{E}^{i}(\mathbf{r}_{dm}) + E_z^i(\mathbf{r}_{cn}). \quad (37)$$

Using (26) and assuming that $\mathbf{E}^i = \hat{\mathbf{z}}E_z^i$, then

$$\frac{I_{cn}(\mathbf{r}_{cn})}{2\pi a\sigma_{cn}} = \varepsilon P_0 F_{z,z}^{e,e}(\mathbf{r}_{cn},\mathbf{r}_{dm})E_z^i(\mathbf{r}_{dm}) + E_z^i(\mathbf{r}_{cn}). \quad (38)$$

If the CN is centered at the origin and the dipole moment at $(x_{dm}, y_{dm} = 0, z_{dm} = 0)$ then

$$F_{z,z}^{e,e}(\mathbf{r}_{cn},\mathbf{r}_{dm}) = F_{z,z}^{e,e}(z) \quad (39)$$

$$= \frac{e^{-jkR}}{4\pi R}\left\{\left(3\left(\frac{z}{R}\right)^2 - 1\right)\frac{1}{R}\left(\frac{1}{\varepsilon R} + j\omega\eta\right) - \left(\left(\frac{z}{R}\right)^2 - 1\right)\omega^2\mu\right\} \quad (40)$$

where the distance between a point z on the tube wall (at $\phi = 0$) and the sphere center is

$$R = \sqrt{z^2 + (a - x_{dm})^2}. \quad (41)$$

Further simplifying, since the CN and the dipole moment are separated by distances on the order of nanometers $E_z^i(\mathbf{r}_{dm}) \simeq E_z^i(\mathbf{r}_{cn}) \simeq E_0$, and so a simple analytical expression for the carbon nanotube current is obtained as

$$I_{cn}(z) = 2\pi a\sigma_{cn}E_0\left(\varepsilon P_0 F_{z,z}^{e,e}(z) + 1\right). \quad (42)$$

This solution could be used in an iterative scheme based on (33) and (34), although (42) itself provides a reasonably accurate closed-form solution away from the tube ends, as shown in Fig. 5 and discussed below. For an isolated carbon nanotube at optical frequencies, an alternative approximate analytical solution based on an iterative approach is presented in [13].

C. Comments on the Model

For an isolated carbon nanotube at optical frequencies, a detailed discussion of the integral equation model used here is provided in [12]. As discussed in that paper and in [31], a comparison between optical Rayleigh scattering measurements and simulation results for a (10, 10) armchair nanotube shows good agreement (up to arbitrarily-normalized amplitudes) using a phenomenological relaxation time of $\tau = 0.01$ ps in (24). It is expected that different nanotubes may require at least slightly different values of τ, although this requires further study, and here $\tau = 0.01$ ps is used.

Furthermore, in this paper we assume a local model of the carbon nanotube, (23). In [9] and [29] an approximate non-local correction is derived, resulting in

$$\left(1 + \xi(\omega)\frac{\partial^2}{\partial z^2}\right)J_z^{cn}(z,\omega) = \sigma_{cn}(\omega)E_z(z,\omega) \quad (43)$$

where $\xi(\omega)$ is a small parameter. This modified form of Ohm's law results from assuming traveling wave behavior of the electric field in the governing transport equation. In [11] the use of (43) for an infinite nanotube antenna in the far infrared and GHz regime yielded results that agreed with the simpler local form (23), and so here we also assume the local relation. However, the strongly inhomogeneous nature of the sphere's near field, coupled with reduced screening in low-dimensional structures, indicates that a nonlocal model coupling electron kinetics and external fields may be useful.

The other part of the model concerns representing the electrically-small polarizable object by its dipole moment. For a single nanosphere having radius less then approximately 10–20 nm, yet greater than 2–3 nm, the dipole moment representation should be valid through the near ultraviolet regime. The upper size limit is dictated by the need for the sphere to be electrically very small, and the lower limit is due to the fact that spheres having sizes below 1–2 nm do not behave as bulk solids. Since the sphere is electrically-small, the electric and magnetic fields obtained from the dipole moment are valid not only far from the sphere, but also on the sphere's surface [28], [32]. Thus, even the situation where the carbon nanotube and the nanosphere are nearly touching can be correctly modeled electromagnetically using the described approach (electronically, however, the local density of states on the carbon nanotube may be modified by the presence of the sphere, although the effect of this interaction is ignored here).

For objects other than spheres, such as electrically-small prolate spheroids, the field on the spheroid surface is not correctly modeled using only dipole moments. In this case one obtains a dipole moment corresponding to an equivalent sphere, outside of which the dipole-moment fields are valid. Since close coupling between the polarizable object and the carbon nanotube is of interest here, the surface field on the object is of primary importance, and, therefore, results are only presented for nanospheres. In this case, the induced electric field at the surface of an isolated nanosphere due to an incident plane wave, computed using the dipole moment, was found to give excellent agreement with the finite-element result in [19]. Note that larger objects could be modeled by partitioning them into N electrically-small spheres and replacing (29) with a system of $N \times N$ equations (this is known as the discrete dipole approximation, see, e.g., [32] and [33]) coupled to the first equation, although this topic isn't investigated here. A good recent review of electromagnetic modeling techniques and associated phenomena for nanostructures is provided in [17].

III. Results

The following results lead to some predictions for the interaction between a carbon nanotube and a plasmonic nanosphere. Fig. 2 shows frequency-dependent material parameters for the objects of interest. The complex conductance (24) for a (9, 0) carbon nanotube ($a = 0.678$ nm) is shown as the upper two curves, corresponding to the left vertical axis, exhibiting optical interband transitions at certain frequencies. The complex permittivity of bulk gold and silver are the lower four curves, corresponding to the right vertical axis, obtained from experimental results [34]. The short vertical arrows at $f = 612$ THz $= F_g$

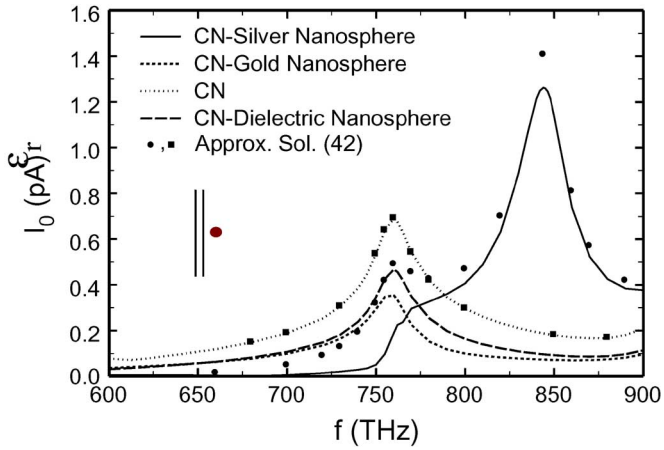

Fig. 3. Current magnitude at the center of a 60 nm long (9, 0) carbon nanotube induced by a 1 V/m uniform plane wave normally incident on a nanotube-nanosphere system (depicted in the insert). The sphere has radius $r = 6$ nm and is centered at $x_{dm} = 3a + r_s$, $y_{dm} = z_{dm} = 0$, and the CN is centered at the origin. For the dielectric nanosphere, $\varepsilon_r = 10$. Also shown is the approximate analytical solution (42), where circles denote the solution for a CN-silver nanosphere system, and squares are for the isolated nanotube.

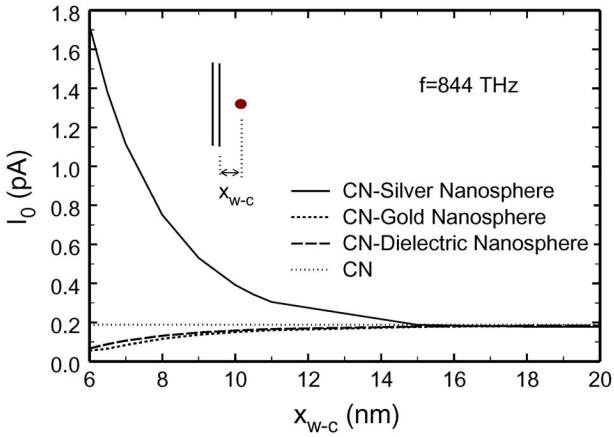

Fig. 4. Current magnitude at the center of a 60 nm long (9, 0) carbon nanotube induced by a 1 V/m uniform plane wave normally incident on the nanotube-sphere system, as the distance between the nearest tube wall and the nanosphere center, x_{w-c}, is varied (as depicted in the insert). The sphere has radius $r_s = 6$ nm and is centered at $x_{dm} = a + x_{w-c}$, $y_{dm} = z_{dm} = 0$, and the CN is centered at the origin. The frequency of the incident plane wave is 844 THz, which corresponds to the plasmon resonance of silver for strong silver sphere-tube coupling.

and $f = 846$ THz $= F_s$ indicate the Fröhlich frequency, where $\mathrm{Re}(\varepsilon_{\mathrm{gold}}) = -2\varepsilon_0$ and $\mathrm{Re}(\varepsilon_{\mathrm{silver}}) = -2\varepsilon_0$, respectively. From (27) it is evident that at these points the nanospheres exhibit plasmonic resonances [27], [32].

It can be seen that silver has lower losses then gold throughout the optical band, and thus one would expect to see stronger plasmonic effects with silver, as is found to be the case. The (9, 0) tube, which is metallic, was chosen for study because the Fröhlich frequency for silver is between two interband transitions of the carbon nanotube, thus decoupling somewhat these different physical effects.

In all of the following results the excitation is an $E_0 = 1$ V/m uniform plane wave normally incident $(\theta = 90°, \phi = 90°)$ on the carbon nanotube-nanosphere system. Fig. 3 shows the current at the center of a 60 nm long (9, 0) carbon nanotube in close proximity to a nanosphere (the tube-sphere system is depicted in the insert). The sphere has radius $r_s = 6$ nm and is centered at $x_{dm} = 3a + r_s$, $y_{dm} = z_{dm} = 0$, and the CN is centered at $x_{cn} = y_{cn} = z_{cn} = 0$. In the figure, results are given for the situation of a carbon nanotube coupled to four different nanospheres: silver, gold, free-space (i.e., no sphere), and an idealized $\varepsilon_r = 10$ dielectric, based on a pulse function, point matching solution of (33) and (34). The smaller peaks near 755 THz are due to interband transitions in the nanotube conductance, as seen in Fig. 2. At this frequency it is evident that the current on the tube center in the presence of the material spheres is smaller then for the isolated CN due to depolarization effects. The peak near 844 THz for the CN-silver nanosphere case is due to the plasmon resonance of the silver sphere (the Fröhlich frequency of 846 THz for bulk silver is shifted slightly due to strong tube-sphere electromagnetic coupling). A similar peak should occur for the CN-gold nanosphere case near $f = 612$ THz, but is not seen due to the relatively strong damping of gold.

Also shown in Fig. 3 is the approximate analytical solution (42). For the isolated carbon nanotube, the analytical solution is in complete agreement with the numerical solution of (33) and (34). For the CN-Silver nanosphere system, the approximate solution is in reasonable agreement with the numerical solution near the plasmon resonance. This is consistent with the development of (42), where the influence of the nanotube current on the nanosphere is neglected, so that the nanosphere is excited only by the incident plane wave, but the nanotube is excited by both the plane wave and the nanosphere. For the sake of clarity of the figure, the approximate solution results for the gold and dielectric sphere are not shown, but reasonable agreement with the numerical solution is obtained. The comparison between the approximate analytical solution (42) and the numerical solution of (33) and (34) is further considered in Fig. 5.

The plasmonic nanosphere obviously has a strong effect on the carbon nanotube current in the case when the sphere and tube are in close proximity (as shown in the figure, at 844 THz the presence of the silver nanosphere increases the center current on the nanotube by an order of magnitude, compared to the isolated tube case). It is well-known that the intense field at the surface of a plasmonic particle decays rapidly with distance, approximately on the order of the sphere radius, and one would expect that the sphere-tube coupling diminishes rapidly with increasing separation. This is indeed found to be the case, as shown in Fig. 4, where the current at the center of the carbon nanotube is shown as the distance between the nearest tube wall and the nanosphere center, x_{w-c}, is varied (as depicted in the insert). The sphere has radius $r_s = 6$ nm and is centered at $x_{dm} = a + x_{w-c}$, $y_{dm} = z_{dm} = 0$, and the CN is centered at the origin. The frequency of the incident plane wave is 844 THz, which corresponds to the plasmon resonance of silver for strong nanotube-nanosphere coupling. As expected, the effect of the silver plasmonic nanosphere on the nanotube diminishes rapidly with separation, and above approximately $x_{w-c} = 15$ nm the material sphere has essentially no effect on the carbon nanotube current.

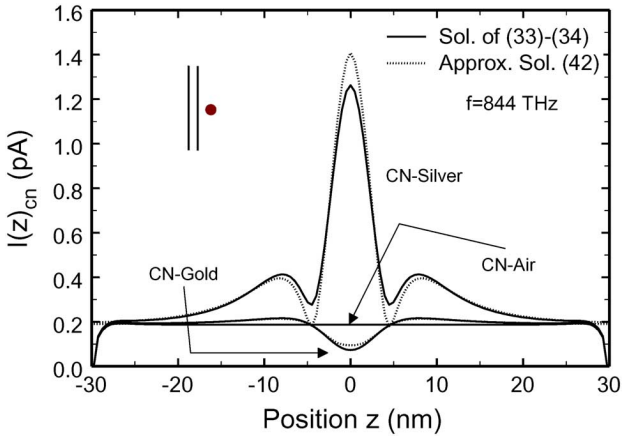

Fig. 5. Current profile (magnitude) on a 60 nm long (9, 0) carbon nanotube induced by a 1 V/m uniform plane wave normally incident on a tube-sphere system (depicted in the insert). The sphere has radius $r_s = 6$ nm and is centered at $x_{dm} = 3a + r_s$, $y_{dm} = z_{dm} = 0$, and the CN is centered at the origin. The peak for the CN-silver sphere is due to the plasmon resonance, and the dip for the CN-gold sphere is due to tangential electric field suppression at the surface of the gold sphere. The approximate analytical solution (42) is also shown.

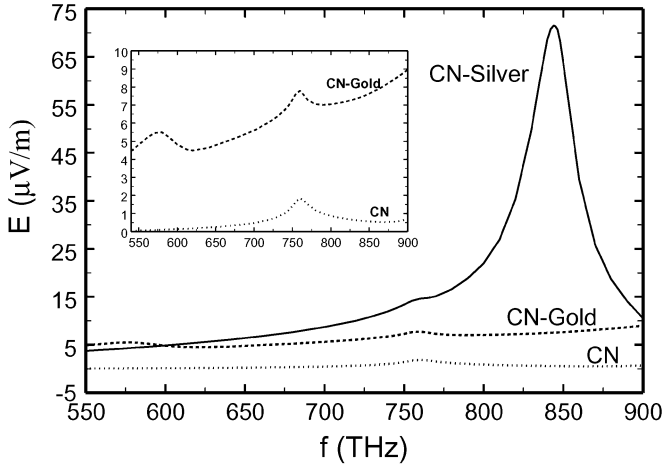

Fig. 6. Magnitude of the backscattered electric field at $y = 10$ μm, $x = z = 0$, from a system consisting of a 60 nm long (9, 0) carbon nanotube and a $r_s = 6$ nm nanosphere. The sphere is centered at $x_{dm} = 3a + r_s$, $y_{dm} = z_{dm} = 0$ and the CN is centered at the origin. The peak for the CN-silver sphere is due to the plasmon resonance of the silver nanosphere, and the small peaks near 755 THz are due to interband transitions on the CN (see Fig. 2). The insert shows a close-up of backscattering from the CN-gold nanosphere system, showing a small peak near the Fröhlich frequency of gold.

Fig. 5 shows the current profile on a 60 nm long (9, 0) carbon nanotube induced by a 1 V/m, 844 THz normally-incident uniform plane wave. The sphere has radius $r_s = 6$ nm and is centered at $x_{dm} = 3a + r_s$, $y_{dm} = z_{dm} = 0$, and the CN is centered at the origin. The peak in the current for the CN-silver sphere is due to the extremely strong near-fields associated with the plasmon resonance of the nanosphere. Since at this frequency the gold sphere does not have a plasmon resonance, the dip for the CN-gold sphere case is due to depolarization effects; the tangential electric field is suppressed at the surface of the gold sphere (the tangential electric field is E_z on the left-side of the sphere near the nanotube, and thus at this point E_z is very small, and would identically vanish if the gold sphere were perfectly conducting). It can also be seen that the approximate analytical solution (42) provides a reasonable closed-form estimate of the nanotube current profile in each case.

Fig. 6 shows the backscattered electric field at $y = 10$ μm, $x = z = 0$, from a system consisting of a 60 nm long (9, 0) carbon nanotube and a $r_s = 6$ nm nanosphere. The sphere is centered at $x_{dm} = 3a + r_s$, $y_{dm} = z_{dm} = 0$ and the CN is centered at the origin. The peak for the CN-silver sphere is due to the plasmon resonance, and a similar, although much smaller plasmonic peak is seen for the gold nanosphere near 575 THz, as shown in the close-up provided in the insert. Scattering from the plasmonic nanosphere is seen to dominate the response of the CN-nanosphere system.

Concerning the numerical results, although a 6 nm radius sphere was assumed here, there would not be any qualitative difference for spheres having radius values in the previously described range. Furthermore, since current is predicted to be strongly damped on CNs at optical frequencies, results will be similar for a wide range of nanotube lengths.

IV. Conclusion

A model has been presented for electromagnetic interactions between a carbon nanotube and an electrically-small material sphere. The carbon nanotube is modeled as an infinitely-thin tube characterized by a full-wave integral equation using a quantum surface conductance, and the electrically-small sphere is modeled by its dipole moment. It is predicted that the presence of a plasmonic nanosphere significantly affects the current on a nearby carbon nanotube, and can be used to induce relatively large currents on the tube in the vicinity of the sphere. An approximate analytical solution for the current induced on a nanotube in the presence of a nanosphere is provided. Backscattering from a carbon nanotube-plasmonic nanosphere system is dominated by the nanosphere, despite the nanotube being electrically much larger.

References

[1] I. Iijima, "Helical microtubules of graphitic carbon," *Nature*, vol. 354, pp. 56–58, 1991.

[2] S. Li, Z. Yu, S. F. Yen, W. C. Tang, and P. J. Burke, "Carbon nanotube transistor operation at 2.6 GHz," *Nano Lett.*, vol. 4, pp. 753–756, 2004.

[3] J. P. Clifford, D. L. John, L. C. Castro, and D. L. Pulfrey, "Electrostatics of partially gated carbon nanotube FETs," *IEEE Trans. Nanotechnol.*, vol. 3, pp. 281–286, Jun. 2004.

[4] A. Naeemi, R. Sarvari, and J. D. Meindl, "Performance comparison between carbon nanotube and copper interconnects for gigascale integration (GSI)," *IEEE Electron Device Lett.*, vol. 26, pp. 84–86, 2005.

[5] A. Naeemi and J. D. Meindl, "Impact of electron-phonon scattering on the performance of carbon nanotube interconnects for GSI," *IEEE Electron Device Lett.*, vol. 26, pp. 476–478, 2005.

[6] Z. Chen, "Nanotubes for nanoelectronics," in *Encyclopedia of Nanoscience and Nanotechnology*, H. S. Nalwa, Ed. Thousand Oaks, CA: American Scientific Publishers, 2004.

[7] Z. Yao, C. Dekker, and P. Avouris, "Electrical transport through single-wall carbon nanotubes," in *Carbon Nanotubes; Topics in Applied Physics*, M. S. Dresselhaus, G. Dresselhaus, and P. Avouris, Eds. Berlin: Springer Verlag, 2001, vol. 80, pp. 147–171.

[8] P. J. Burke, S. Li, and Z. Yu, "Quantitative theory of nanowire and nanotube antenna performance," *IEEE Trans. Nanotechnol.*, vol. 5, pp. 314–334, Jul. 2006.

[9] G. Ya. Slepyan, S. A. Maksimenko, A. Lakhtakia, O. Yevtushenko, and A. V. Gusakov, "Electrodynamics of carbon nanotubes: Dynamic conductivity, impedance boundary conditions, and surface wave propagation," *Phys. Rev. B*, vol. 60, pp. 17136–17149, Dec. 1999.

[10] G. W. Hanson, "Fundamental transmitting properties of carbon nanotube antennas," *IEEE Trans. Antennas. Propag.*, vol. 53, pp. 3426–3435, Nov. 2005.
[11] G. W. Hanson, "Current on an infinitely-long carbon nanotube antenna excited by a gap generator," *IEEE Trans. Antennas Propag.*, vol. 54, pp. 76–81, Jan. 2006.
[12] J. Hao and G. W. Hanson, "Infrared and optical properties of carbon nanotube dipole antennas," *IEEE Trans. Nanotechnol.*, vol. 5, pp. 766–775, Nov. 2006.
[13] G. Ya. Slepyan, M. V. Shuba, S. A. Maksimenko, and A. Lakhtakia, "Theory of optical scattering by achiral carbon nanotubes and their potential as optical nanoantennas," *Phys. Rev. B*, vol. 73, p. 195416, 2006.
[14] Y. Wang, K. Kempa, B. Kimball, J. B. Carlson, G. Benham, W. Z. Li, T. Kempa, A. Rybczynski, and Z. F. Ren, "Receiving and transmitting light-like radio waves: Antenna effect in arrays of aligned carbon nanotubes," *Appl. Phys. Lett.*, vol. 85, pp. 2607–2609, Sep. 2004.
[15] K. J. Webb and J. Li, "Resonant slot optical guiding in metallic nanoparticle chains," *Phys. Rev. B*, vol. 72, p. 201402(R), 2005.
[16] J. C. Weeber, A. Dereux, Ch. Girard, G. Colas des Francs, J. R. Krenn, and J. P. Goudonnet, "Optical addressing at the subwavelength scale," *Phys. Rev. E*, vol. 62, p. 7381, 2000.
[17] C. Girard, "Near fields in nanostructures," *Rep. Prog. Phys.*, vol. 68, pp. 1883–1933, 2005.
[18] M. J. Kogan, N. G. Bastus, R. Amigo, D. Grillo-Bosch, E. Araya, A. Turiel, A. Labarta, E. Giralt, and V. F. Puntes, "Nanoparticle-mediated local and remote manipulation of protein aggregation," *Nano Lett.*, vol. 6, pp. 110–115, 2006.
[19] Y. C. Martin, H. F. Hamann, and H. K. Wickramasinghe, "Strength of the electric field in apertureless near-field optical microscopy," *J. Appl. Phys.*, vol. 89, pp. 5774–5778, 2001.
[20] N. Calander and M. Willander, "Theory of surface-plasmon resonance optical-field enhancement at prolate spheroids," *J. Appl. Phys.*, vol. 92, pp. 4878–4884, 2002.
[21] J. Aizpurua, G. W. Bryant, L. J. Richter, F. J. Garcia de Abajo, B. K. Kelly, and T. Mallouk, "Optical properties of coupled metallic nanorods for field-enhanced spectroscopy," *Phys. Rev. B.*, vol. 71, p. 235420, 2005.
[22] R. Saito, G. Dresselhaus, and M. S. Dresselhaus, *Physical Properties of Carbon Nanotubes*. London, U.K.: Imperial College Press, 2003.
[23] W. C. Chew, *Waves and Fields in Inhomogeneous Media*. New York: IEEE Press, 1990.
[24] G. W. Hanson and A. B. Yakovlev, *Operator Theory for Electromagnetics: An Introduction*. New York: Springer, 2002.
[25] G. W. Hanson and C. E. Baum, "Asymptotic analysis of the natural system modes of coupled bodies in the large separation, low-frequency regime," *IEEE Trans. Antennas Propag.*, vol. 47, pp. 101–111, Jan. 1999.
[26] A. D. Yaghjian, "Electric dyadic Green's functions in the source region," *IEEE Proc.*, vol. 68, pp. 248–263, Feb. 1980.
[27] C. F. Bohren and D. R. Huffmann, *Absorption and Scattering of Light by Small Particles*. New York: Wiley, 1983.
[28] R. F. Harrington, *Time-Harmonic Electromagnetic Fields*. New York: McGraw-Hill, 1961.
[29] S. A. Maksimenko and G. Ya. Slepyan, "Electrodynamic properties of carbon nanotubes," in *Electromagnetic Fields in Unconventional Materials and Structures*, O. N. Singh and A. Lakhtakia, Eds. New York: Wiley, 2000.
[30] S. A. Maksimenko and G. Y. Slepyan, "Nanoelctromagnetics of low-dimensional structures," in *The Handbook of Nanotechnology—Nanometer Structures—Theory, Modeling, and Simulation*, A. Lakhtakia, Ed. Bellingham, WA: Spie Press, 2004.
[31] J. Hao and G. W. Hanson, "Electromagnetic scattering from finite-length metallic carbon nanotubes in the lower IR bands," *Phys. Rev. B*, vol. 74, p. 035119.
[32] K. L. Kelly, E. Coronado, L. L. Zhao, and G. C. Schatz, "The optical properties of metal nanoparticles: the influence of size, shape, and dielectric environment," *J. Phys. Chem. B*, vol. 107, pp. 668–677, 2003.
[33] E. Hao and G. C. Schatz, "Electromagnetic fields around silver nanoparticles and dimers," *J. Chem. Phys.*, vol. 120, pp. 357–366, 2004.
[34] P. B. Johnson and R. W. Christy, "Optical constants of the noble metals," *Phys. Rev. B*, vol. 6, pp. 4370–4379, Jul. 1972.

George W. Hanson (S'85–M'91–SM'98) was born in Glen Ridge, NJ, in 1963. He received the B.S.E.E. degree from Lehigh University, Bethlehem, PA, the M.S.E.E. degree from Southern Methodist University, Dallas, TX, and the Ph.D. degree from Michigan State University, East Lansing, in 1986, 1988, and 1991, respectively.

From 1986 to 1988, he was a Development Engineer with General Dynamics in Fort Worth, TX, where he worked on radar simulators. From 1988 to 1991, he was a Research and Teaching Assistant in the Department of Electrical Engineering at Michigan State University. He is currently Associate Professor of electrical engineering and computer science at the University of Wisconsin in Milwaukee. His research interests include nanoelectromagnetics, mathematical methods in electromagnetics, electromagnetic wave phenomena in layered media, integrated transmission lines, waveguides, and antennas, and leaky wave phenomena.

Dr. Hanson is a member of URSI Commission B, Sigma Xi, and Eta Kappa Nu. In 2006 he received the S. A. Schelkunoff Best Paper Award from the IEEE Antennas and Propagation Society. He is an Associate Editor for the IEEE TRANSACTIONS ON ANTENNAS AND PROPAGATION.

Paul Smith, photograph and biography not available at the time of publication.